

Postprint of: Ordyszewska A., Szyrkiewicz N., Ponikiewski Ł., Scheer M., Pikies J., Grubba R.: Syntheses and Structures of Transition Metal Complexes with Phosphanylphosphinidene Chalcogenide Ligands. **INORGANIC CHEMISTRY**, Vol. 58, iss. 12 (2019), pp. 7905-7914, DOI: [10.1021/acs.inorgchem.9b00594](https://pubs.acs.org/doi/10.1021/acs.inorgchem.9b00594)

The Syntheses and Structures of Transition Metal Complexes with Phosphanylphosphinidene Chalcogenide Ligands

*Anna Ordyszewska^[a], Natalia Szyrkiewicz^[a], Łukasz Ponikiewski^[a], Manfred Scheer^[b], Jerzy
Pikies^[a] and Rafał Grubba^{*[a]}*

[a] Department of Inorganic Chemistry, Faculty of Chemistry, Gdańsk University of
Technology, 11/12 Gabriela Narutowicza Str. 80-233 Gdańsk, Poland

[b] Institut für Anorganische Chemie, Universität Regensburg, Universitätsstrasse 31,
Regensburg D-93040, Germany

*rafal.grubba@pg.edu.pl

KEYWORDS: P-donor ligands, phosphinidene, tungsten, chalcogens, reactivity

ABSTRACT

The reactivity of the phosphanylphosphinidene complex $[(\text{DippN})_2\text{W}(\text{Cl})(\eta^2\text{-P-P}t\text{Bu}_2)]^-$ (**1**) towards chalcogens (Ch= Se, S) was studied. Reactions of stoichiometric amounts of **1** with chalcogens in DME yielded monomeric tungsten complexes with phosphanylphosphinidene chalcogenide ligands of the formula $t\text{Bu}_2\text{P-P-Ch}$ (Ch = Se (in **2**) and S (in **5**)), which can be regarded as products of the addition of a chalcogen atom to a P=W bond in starting complex **1**. The dissolution of selenophosphinidene complex **2** in nondonor solvents led to the formation of a dinuclear complex of tungsten (**3**) bearing a $t\text{Bu}_2\text{P}(\text{Se})\text{-P}$ ligand together with $[t\text{BuSe}_2\text{Li}(\text{dme})_2]_2$ and polyphosphorus species. Under the same reaction conditions, thiophosphinidene complex **5** dimerized via the formation of transient complex **7**, possessing a thiotetraphosphane-diido moiety $t\text{Bu}_2\text{P}(\text{S})\text{-P-P-P}t\text{Bu}_2$. The elimination of the $t\text{Bu}_2\text{PS}$ group from **7** yielded stable dinuclear tungsten complex **8** with an unusual phosphinidene $t\text{Bu}_2\text{P-P-P}$ ligand. The reaction of **1** with excess chalcogen led to the cleavage of the P-P bond in the $t\text{Bu}_2\text{P-P}$ ligand and the formation of $[(\text{DippN})_2\text{W}(\text{PCh}_4)]_2^{2-}$ and $[t\text{BuCh}_2\text{Li}(\text{dme})_2]_2$. The isolated compounds were characterized by NMR spectroscopy and X-ray crystallography. Furthermore, the calculated geometries of the free selenophosphinidenes, $t\text{Bu}_2\text{P-P-Se}$ and $t\text{Bu}_2\text{P}(\text{Se})\text{-P}$, were compared with their geometries when serving as ligands in complexes **2** and **3**.

1. INTRODUCTION

Thus far, phosphinidenes have generally been regarded as short-lived intermediates. Recently, Bertrand *et al.*¹ designed and synthesized a first isolable singlet phosphanylphosphinidene RP with a very bulky substituent. This R group displays very strong π -donor properties and kinetically stabilizes the resulting phosphanylphosphinidene due to the substantial steric hindrance of this group. Generally, phosphinidene moieties can be trapped by transition metal complexes^{2–7} or stabilized as adducts with an appropriate Lewis base as stable carbenes^{8,9} or phosphines.^{7,8,10} The phosphine adducts of phosphinidenes show significant Wittig-like reactivity and can be used as phosphinidene sources.^{11–13} Phosphinidene chalcogenides are generally very reactive transient species, and to the best of our knowledge, no free phosphinidene chalcogenides are known. However, they can be stabilized as adducts with carbenes or as ligands in the coordination sphere of transition metals. Very recently, Ragogna *et al.* generated R–P=X phosphinidene chalcogenides from four-membered heterocycles (R-P(μ_2 -S)₂P-R, R = 2,6-Mes₂C₆H₃).^{14,15} The monomeric R–P=S unit can be stabilized as an adduct with a stable carbene.¹⁴ There are two main methods of accessing complex-stabilized phosphinidene chalcogenides. The first method is to generate the related R–P=X phosphinidene chalcogenide and trap it with a transition metal.^{13–21} Trapping experiments have revealed that R–P=X displays singlet-carbene-like reactivity.¹⁶ The second method of accessing complexes with phosphinidene chalcogenide ligands is to oxidize complexes with low-valent phosphorus ligands with free chalcogens or with chalcogen sources. Reports on the oxidation of monomeric complexes are rather rare. Cummins reported the oxidation of the terminal phosphide complex [$\{R(Ar)N\}_3Mo\equiv P$] to yield [$\{R(Ar)N\}_3Mo=P=X$] (X = O, S).¹⁷ The Scheer group synthesized the terminal complexes [(N₃N)W(ES)] (N₃N=N(CH₂CH₂NSiMe₃)₃; E = P or As) via reactions of [(N₃N)W \equiv E] with



cyclohexene sulfide.¹⁸ The reaction of $[\text{Cp}(\text{OC})_2\text{Fe-P}=\text{PMes}^*]$ with S yields $[\text{Cp}(\text{OC})_2\text{Fe-P}(\text{S})=\text{PMes}^*]$.¹⁹ The sulfurization of the phosphonium complexes $[\text{Cp}(\text{OC})_2\text{W}=\text{P}\{\text{N}(\text{SiMe}_3)_2\}(\text{Ph})]$ ²⁰ or $[(\text{C}_5\text{R}_5)(\text{OC})_2\text{W}=\text{P}(\text{H})t\text{Bu}]$ ²¹ leads to the addition of an S atom to the M=P bond, while a similar reaction with the Fe(II) phosphido complex $[\text{Cp}(\text{OC})_2\text{Fe-PPh}_2]$ yields $[\text{Cp}(\text{OC})_2\text{Fe-P}(\text{S})\text{Ph}_2]$.²² The addition of H_2O to $[\text{dppe}_2\text{ReCl}(\text{P}=\text{C}t\text{Bu})]$ gives the complex $[\text{dppe}_2\text{ReCl}(\text{P}(\text{O})-\text{CH}_2t\text{Bu})]$ with a phosphinidene oxide ligand.²³ Ruiz *et al.* reported the formation and properties of the anionic complex $[(\eta^5-\text{C}_5\text{H}_5)(\text{OC})_2\text{Mo}=\text{P}(\text{O})\text{Ar}]^-$ (Ar = 2,4,6- $t\text{Bu}_3\text{C}_6\text{H}_2$).²⁴ The electronic structure of this kind of complex with a phosphinidene oxide ligand has been discussed.²⁵ Such complexes can be further oxidized by sulfur with concomitant incorporation of an S atom across the Mo=P bond yielding the thioxophosphorane complex $[\text{Cp}(\text{OC})_2\text{Mo}\{\kappa^2\text{-SP}(\text{O})\text{Ar}\}]^-$.²⁶ The nucleophilicity of this complex and its oxygen analog, $[\text{Cp}(\text{OC})_2\text{Mo}\{\kappa^2\text{-OP}(\text{O})\text{Ar}\}]^-$, towards soft and hard electrophiles has also been investigated.²⁷

The reactivity of dinuclear complexes bearing low-valent phosphorus ligands towards chalcogens has been studied in more detail.²⁸ The oxidation of the dinuclear rhenium complex $[\text{Cp}^*(\text{OC})_2\text{Re}]_2$ in the presence of $t\text{BuC}\equiv\text{P}$ yields a dinuclear complex with a phosphinidene oxide ligand.²⁹ Dinuclear Mo and W phosphonium complexes react with S and Se via the addition of the chalcogen to the M=P bond.³⁰ Dinuclear phosphinidene-bridged scandium complexes react with Se, Te or $\text{R}_3\text{P}=\text{X}$ (S, Se), which oxidizes two Ar-P units to form a bridging μ_2 diphosphene ligand, Ar-P=P-Ar, containing a bridging $\mu_2\text{-X}$ moiety between two scandium atoms.³¹ The electron-rich nucleophilic dimeric platinum phosphinidene complex $[(\text{dppe})\text{Pt}(\mu\text{-PMes})]_2$ can be oxidized in air to $[(\text{dppe})\text{Pt}\{\mu\text{-P}(\text{O})\text{Mes}\}]_2$. Sulfur cleaves the Pt-P bonds, yielding the monomeric trithioxophosphorane complex $[(\text{dppe})\text{Pt}(\text{S}_3\text{PMes})]$.³² The synthesis and reactivity of dinuclear $\mu\text{-PR}$ -bridged complexes towards various electrophiles were systematically studied by the Ruiz

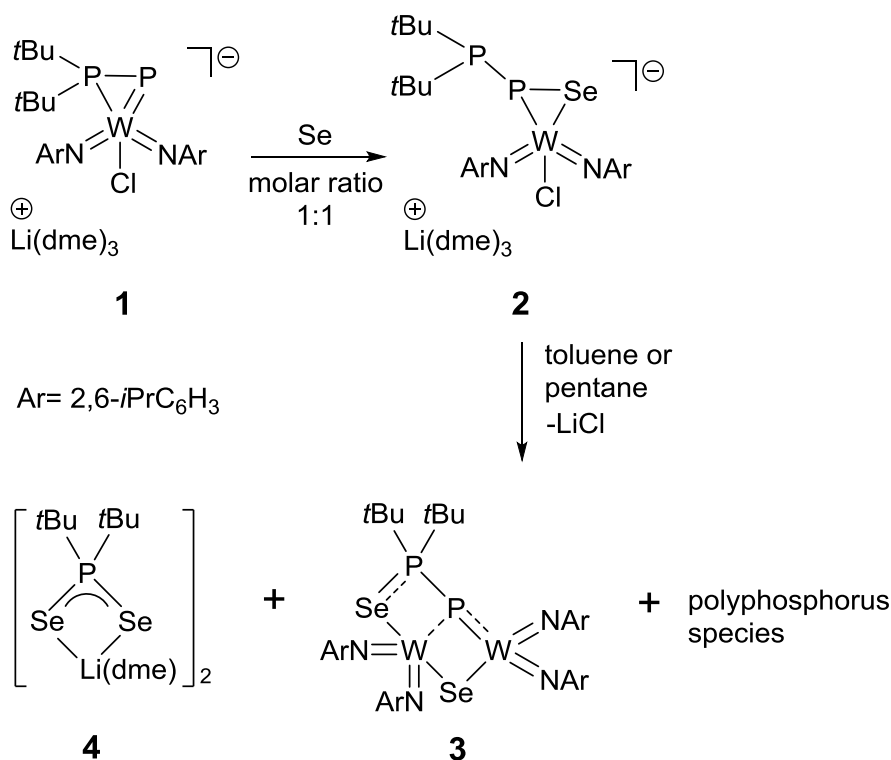
group. $[\text{Fe}_2\text{Cp}_2(\mu\text{-PCy})(\mu\text{-CO})(\text{CO})_2]$ reacts rapidly with O_2 or S_8 yielding $[\text{Fe}_2\text{Cp}_2\{\mu\text{-P(E)R}\}(\mu\text{-CO})(\text{CO})_2]$ where $\text{E} = \text{O}, \text{S}$ and $\text{R} = \text{Cy}, \text{Ph}$.^{33,34} The reactivity of the similar but sterically overcrowded complex $[\text{Fe}_2\text{Cp}_2(\mu\text{-PMes}^*)(\mu\text{-CO})(\text{CO})_2]$ differs significantly.³⁵ This compound is less stable and readily undergoes hydrogen addition. The unsymmetrical thiophosphinidene complex $[\text{Mo}_2\text{Cp}_2\{\mu\text{-}\kappa^2_{\text{P,S}}:\kappa^1_{\text{P}},\eta^6\text{-SPMes}^*\}(\text{CO})_2]$ reacts with metal carbonyls by cleavage of the P-S bond, which represents a new method for accessing heterometallic complexes with bridging phosphinidene ligands.^{36–38} Considering the influence of spectator ligands,³⁹ the majority of the above-discussed phosphinidene complexes should be regarded as nucleophilic. The sulfurization of the electrophilic $[\text{Mn}_2(\text{CO})_8(\mu\text{-PR})]$ complexes ($\text{R} = \text{TMP}, i\text{Pr}_2\text{N}$) follows a different pathway and yields products in which the P=S moieties are side-on bound to the metal centers.⁴⁰ Recently, we started to study the reactivity of the anionic phosphanylphosphinidene W(VI) complex $[(\text{DippN})_2\text{W}(\text{Cl})(\eta^2\text{-P-PtBu}_2)]\text{Li}\cdot 3\text{DME}^{41}$ towards nucleophilic and electrophilic reagents^{42,43} and reported a DFT study on the bonding properties of transition metal complexes with phosphanylphosphinidene ligands.⁴⁴ Generally, the $\text{R}_2\text{P-P}$ ligands coordinate side-on to the metal center, but the kind of bonding substantially depends on the metal (early vs. late TMs). Due to the lack of studies on the reactivity of nucleophilic phosphanylphosphinidene complexes towards chalcogens, we report herein the first such studies involving $[(\text{DippN})_2\text{W}(\text{Cl})(\eta^2\text{-P-PtBu}_2)]^-$.

2. RESULTS AND DISCUSSION

The phosphanylphosphinidene complex $[(\text{DippN})_2\text{W}(\text{Cl})(\eta^2\text{-P-PtBu}_2)]$ (**1**) reacts with gray selenium at a molar ratio of 1:1 under mild conditions. Monitoring the reaction progress by ^{31}P NMR spectroscopy revealed the quantitative formation of a single product (**2**) after six hours of stirring at room temperature (Scheme 1). Newly formed **2** displays an AX pattern in the ^{31}P NMR



spectrum with resonances at 55.8 ppm and -30.7 ppm ($^1J_{PP} = -262$ Hz). Additionally, the latter resonance exhibits W and Se satellites (d, $^1J_{PW} = 57$ Hz, $^1J_{PSe} = 160$ Hz), confirming the presence of the *t*Bu₂P-P-Se ligand in the coordination sphere of the tungsten. The formation of **2** occurs via the addition of one chalcogen atom to the W=P double bond. This type of reactivity is standard for nucleophilic complexes and was previously found in the case of bridging nucleophilic Mo phosphinidene complexes [Mo₂Cp₂{ μ -PH, η^6 -HMes*}(CO)₂] or [Mo₂Cp₂{ μ - κ^1 : κ^1 , η^6 -PMes*}(CO)₂]³⁶ as well as in the case of W phosphonium complexes [Cp(OC)₂W=P{N(SiMe₃)₂}(Ph)]²⁰ or [(C₅R₅)(OC)₂W=P(H)*t*Bu].²¹ Complex **2** was isolated in a moderate yield (48%) as large orange crystals via crystallization from a DME solution layered with pentane at +4°C. The X-ray structure of **2** clearly shows the presence of a phosphanylphosphinidene selenide ligand (Figure 1).



Scheme 1. The reaction of **1** with an equimolar amount of gray selenium.

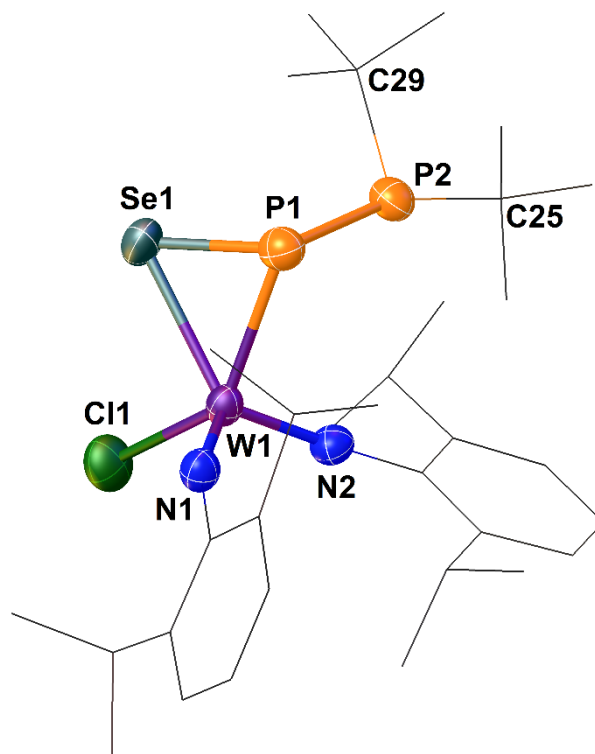


Figure 1. Molecular structure of the anion of complex **2**. Ellipsoids are shown at 50% probability. H atoms are omitted for clarity. Selected bond lengths (Å) and angles (°): P1-W1 2.507(1), Se1-W1 2.5512(6), P1-Se1 2.239(2), P1-P2 2.247(2), C25-P2 1.904(6), C29-P2 1.904(6), P2-P1-Se1 104.47(6), P2-P1-W1 103.33(6), P1-Se1-W1 62.71(4), Se1-P1-W1 64.75(4), and P1-W1-Se1 52.53(3).

The *t*Bu₂P-P-Se moiety is bound to the metal center via the P1 and Se1 atoms. In contrast to starting material **1**, the phosphanyl *t*Bu₂P group does not coordinate to the tungsten. The W atom is formally pentacoordinated, and a three-membered ring involving the P1, Se1 and W1 atoms was formed as a result of the addition of a Se atom into the P=W double bond of starting phosphanylphosphinidene complex **1**. The P1-W1 distance in **2** is significantly longer than the corresponding distance in **1** (2.507(1) Å vs. 2.4056(11) Å),⁴² suggesting a single-bond character. Similarly, the Se1-W1 (2.5512(6) Å), P1-Se1 (2.239(2) Å) and P1-P2 (2.247(2) Å) bond lengths are typical for single covalent bonds (sum of the single bond covalent radii for Se and W = 2.53 Å, P and Se = 2.27 Å, P and P = 2.22 Å).⁴⁵ The P1 and P2 atoms are in pyramidal geometries with Σ272.5° and Σ310°, respectively.



DFT computations were performed to further elucidate the structural features of **2**. The calculated Mayer bond orders for P1-P2, P1-Se1, P1-W1 and Se1-W1 are between 0.840 and 0.951 and confirm the single-bond character of these bonds. Moreover, they essentially show σ -bond character. These results, which were obtained based on chalcogenophosphinidene ligands, exclude ethylene-like coordination of the P=S bond to the metal center.^{22,40,46–48} Hirshfeld population analysis indicates that the P-P bond in **2** is less polarized than the P-P bond in **1**, with P2 being positively charged both in **1** (+0.124)⁴⁴ and **2** (+0.122) and P1 being negatively charged in **1** (-0.177)⁴⁴ and almost neutral in **2** (-0.020). The P1-Se1 bond is polarized towards Se1 with a significant negative charge on this atom (-0.177). As expected, there is a large positive charge on the W1 atom (+0.412). The analysis of the natural bonding orbitals (NBO) reveals the presence of a lone pair of electrons on P1 and on P2 and two lone pairs on Se1. The calculations of the condensed Fukui functions suggest that **2** has nucleophilic properties; unlike in **1**, the nucleophilic center was not P1 but instead was on Se1, which showed a value of $f_k^- = 0.149$.

Complex **2** is fairly stable in DME solution. However, the dissolution of **2** in toluene or pentane leads to the elimination of LiCl and subsequent rearrangement, as shown in Scheme 1. The ³¹P NMR spectra of this solution revealed the formation of dimeric complex **3** together with [(*t*Bu₂PSe₂Li)dme]₂ (**4**) and unidentified polyphosphorus compounds. These observations suggest that the dimerization of **2** to **3** is related to the elimination of the *t*Bu₂P-P moiety, which further reacts to generate polyphosphorus species and compound **4**. The ³¹P NMR spectrum confirmed the presence of compound **3** based on the AX pattern with resonances at 139.1 ppm (P-phosphinidene) and at 88.8 ppm (P-phosphanyl) (¹J_{PP} = -451 Hz). Similar to that of **2**, the signal of the P-phosphinidene atom reveals W satellites (¹J_{PW} = 111 Hz). However, in contrast to **2**, this P atom does not couple with the Se atom, while the signal of the P-phosphanyl atom has Se satellites (¹J_{PSe}



= 370 Hz). All these data indicate that **3** contains a *t*Bu₂P(Se)P ligand. Complexes **3** and **4** were investigated by X-ray crystallography (Figure 2 and Figure S1).

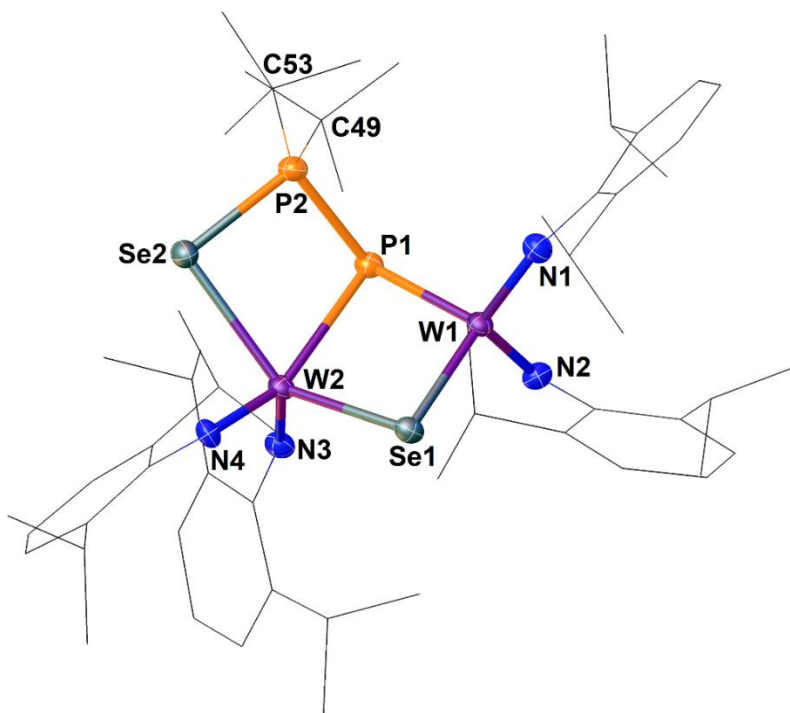
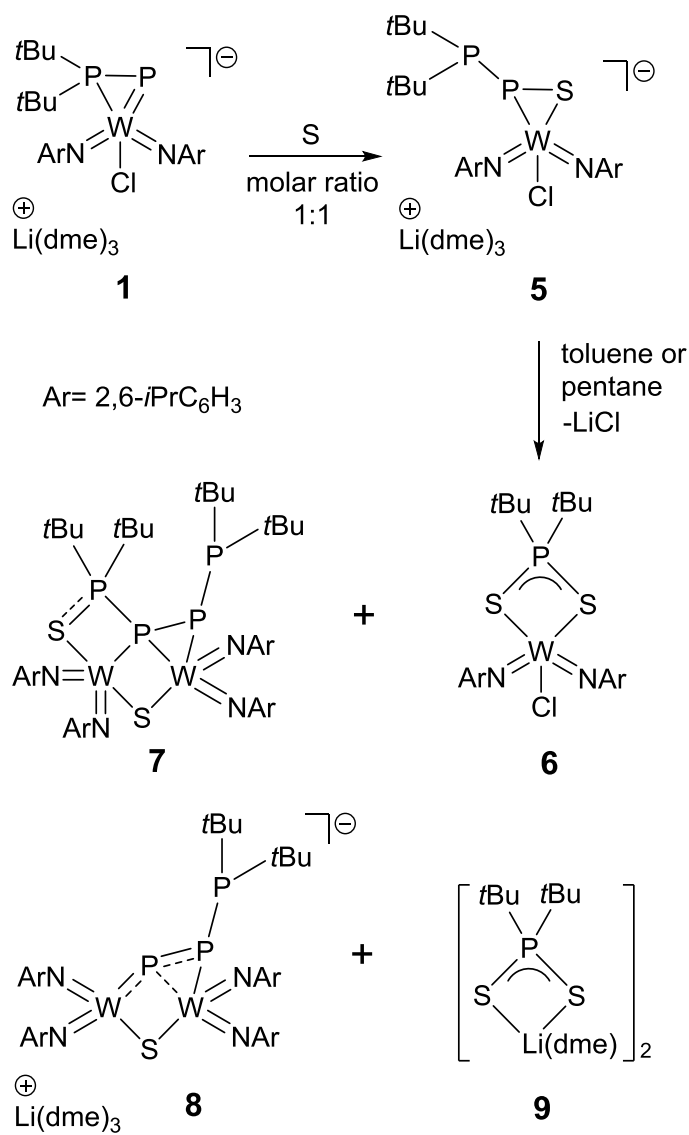


Figure 2. Molecular structure of **3**. Ellipsoids are shown at 50% probability. H atoms are omitted for clarity. Selected bond lengths (Å) and angles (°): Se1-W1 2.4466(5), Se1-W2 2.5153(6), Se2-W2 2.5956(7), P1-W1 2.346(1), P1-W2 2.706(1), P1-P2 2.160(2), P2-Se2 2.202(2), P2-C49 1.876(7), P2-C53 1.891(6), P1-P2-Se2 94.24(7), W1-Se1-W2 82.92(2), W2-Se2-P2 92.12(4), W1-P1-W2 80.79(4), P2-P1-W1 117.08(7), P2-P1-W2 90.09(6), and P2-Se2-W2 92.12(4).

The X-ray structure of **3** confirmed the NMR results and showed that the P1-phosphinidene atom of the *t*Bu₂P2(Se2)P1 ligand and Se1 link the two metal centers. The selenide bridge is asymmetric, with Se1-W1 and Se1-W2 distances differing by 0.0687 Å. Additionally, Se2 of the *t*Bu₂P(Se)P ligand coordinates to W2 with an even longer Se2-W2 distance than the one observed in the case of the selenide Se1 ligand, indicating this bond possesses substantial single-bond character. The W1 atom exhibits distorted tetrahedral geometry, whereas the W2 atom possesses highly distorted bipyramidal trigonal geometry. Interestingly, the P1-W1 distance is very short (2.346(1) Å), even shorter than in parent compound **1** (2.4056(11) Å)⁴², suggesting some multiple-bond character.

The P1-W2 bond is very long (2.706(1) Å), which indicates a weak interaction between the P1 atom and the W2 metal center. The values of the calculated Mayer bond orders for the P1-W1 and P2-W2 bonds are 1.28 and 0.57, respectively, and support this interpretation. The P1-P2 bond distance of 2.160(2) Å has an intermediate value between the analogous distances in **1** (2.1065(17) Å)⁴² and **2** (2.247(2) Å). Moreover, the P2-Se2 distance (2.202(2) Å) is substantially shorter than the expected value for a P-Se single bond, which suggests some multiple-bond character (sum of single bond covalent radii for P and Se = 2.27 Å; sum of double bond covalent radii for P and Se = 2.09 Å).^{45,49} P2 shows distorted tetrahedral geometry, while the coordination geometry at P3 is pyramidal with $\Sigma 288.0^\circ$. To the best of our knowledge, **2** and **3** are the first examples of transition-metal complexes with coordinated phosphanylphosphinidene chalcogenide ligands.

Moreover, the stoichiometric reaction of phosphanylphosphinidene complex **1** with elemental sulfur was investigated. The DME solution of **1** reacts smoothly with solid sulfur at room temperature. This reaction yields several products, and the results strongly depend on the reaction conditions (Scheme 2). Nevertheless, ³¹P NMR studies of the reaction solutions shed light on a possible reaction pathway. Initially, the ³¹P NMR spectrum of the reaction solution reveals two products. The main product shows an AX spin pattern with resonances at 54.4 ppm and at –36.9 ppm (¹J_{PP} = –259 Hz). Taking into account the ³¹P NMR data for selenophosphanylphosphinidene complex **2** (AX spin pattern: 55.8 ppm, –30.7 ppm, ¹J_{PP} = –264.8 Hz), this pattern can be assigned to the monomeric thiophosphanylphosphinidene complex [(DippN)₂W(Cl)(η²-PS-PtBu₂)][–] (**5**) resulting from the addition of a sulfur atom to the P1=W1 double bond of **1**.



Scheme 2. The reaction of **1** with an equimolar amount of sulfur.

The second minor product exhibits a singlet in the ^{31}P NMR spectrum at 115.0 ppm, which can be unambiguously assigned to complex **6**, indicating that sulfur is able to cleave a P-P bond of low-valent phosphorus compounds.⁵⁰ Compared to seleno-derivative **2**, thiophosphanylphosphinidene complex **5** seems to be less stable in solution and tends to dimerize, yielding complex **7** (which shows an AMRZ spin pattern). The formation of **7** is accelerated if DME is replaced with toluene or pentane, as these solvents favor the elimination of LiCl from **5**. The growth of the signals of **7**

is accompanied by the appearance of a new set of resonances (AMX pattern) attributable to dinuclear complex **8** with a *t*Bu₂P-P-P ligand. Notably, in the ³¹P NMR spectrum of **8**, the signal attributed to the P1 atom is shifted dramatically downfield ($\delta = 388.7$ ppm), revealing its phosphinidene character. **8** can be regarded as a product of the elimination of a *t*Bu₂PS fragment from **7**, which can then be captured by **6** and **9** containing dithiophosphinate moieties [*t*Bu₂PS₂][−]. **5** could not be isolated because of its instability in solution. However, we were able to isolate intermediate compound **7**, the phosphinidene complex **8** and the dithiophosphinate compounds **6** and **9** as crystals. Their X-ray structures are depicted in Figures 3, 4, S2 and S3, respectively.

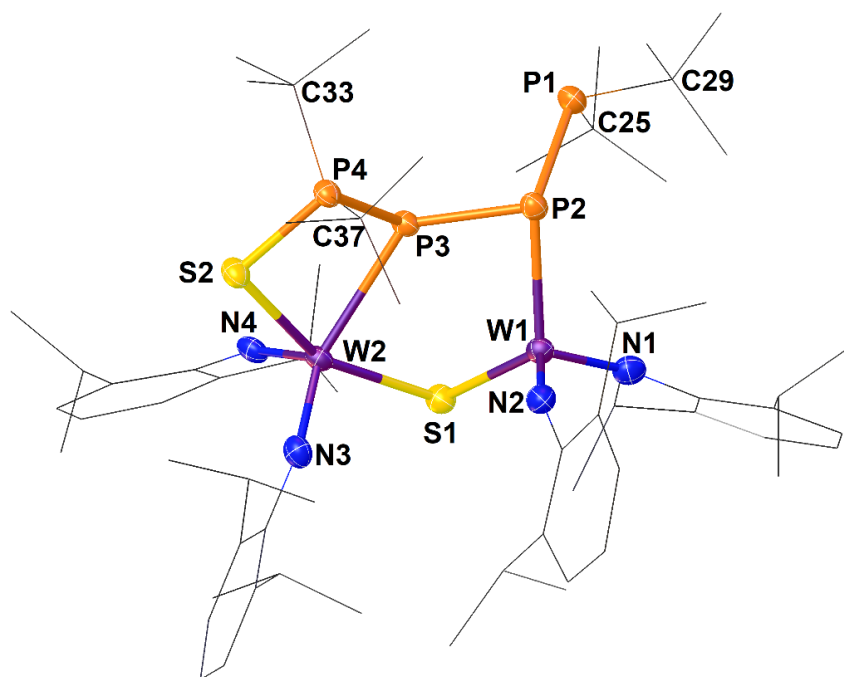


Figure 3. Molecular structure of **7**. Ellipsoids are shown at 50% probability. H atoms are omitted for clarity. Selected bond lengths (Å) and angles (°): P2-W1 2.435(2), S1-W1 2.319(2), P3-W2 2.641(1), S1-W2 2.396(2), S2-W2 2.501(2), P4-S2 2.039(2), P1-P2 2.202(2), P2-P3 2.173(2), P3-P4 2.157(3), P1-C29 1.891(8), P1-C25 1.898(9), P4-C33 1.867(6), P4-C37 1.861(8), P1-P2-P3 104.1(1), P2-P3-P4 110.7(1), W1-S1-W2 100.24(6), W2-S2-P4 96.40(8), P2-W1-S1 117.58(6), P3-P2-W1 81.64(7), P2-P3-W2 131.09(9), P3-W2-S2 74.30(5), P4-P3-W2 89.61(7), P3-P4-S2 95.51(9), and P3-W2-S1 82.14(5).

The X-ray structure of **7** reveals the formation of a thiotetraphosphane-diido ligand in the coordination sphere of two tungsten atoms. This group acts as a tridentate bridging ligand, where

P2 coordinates to the W1 and P3 atoms, and S2 coordinates to the W2 atom. Additionally, two metal centers are connected by S1 of the sulfido ligand. Similar to dinuclear complex **3**, the W1 metal center has a tetrahedral geometry, whereas W2 adopts a highly distorted bipyramidal trigonal geometry. The P1, P2 and P3 atoms all show pyramidal geometries. The P-P distances in **7** are between 2.157(3) and 2.202(2) Å, indicating the primarily single-bond character of these bonds. However, some π -interactions along the P2-P3-P4 bonds are also possible. The P-W distances are comparable to those observed for dinuclear tungsten complexes containing the *catena*-polyphosphorus ligands.^{42,51} The P4-S2 bond length (2.039(2) Å) suggests π -interactions contribute significantly (sum of single bond covalent radii for P and S = 2.14 Å; sum of double bond covalent radii for P and S = 1.96 Å).^[45,49]

The X-ray structure of anionic complex **8** is in accordance with its spectroscopic parameters (see the experimental section). This complex crystallizes with two independent molecules in a unit cell with the two entities having very similar parameters (only one anion is presented in Figure 4). This complex contains the triphosphorus ligand *t*Bu₂P3-P2-P1, where three different types of P atoms can be identified: phosphinidene P1, phosphido P2 and phosphanyl P3. Such a low-valent polyphosphorus ligand with diverse P atoms has never before been described in the literature. Interestingly, some of the structural motifs of complex **8** are similar to those of selenophosphinidene complex **3**. In both complexes, the four-membered rings (W1-Ch-W2-P1, Ch = Se or S) are slightly folded along the W1-W2 vector, with very short P1-W1 bond lengths, which suggests a π -bonding contribution. Both complexes display very long P1-W2 distances. In contrast to complex **3**, the *t*Bu₂PCh group in **8** is replaced by a *t*Bu₂P3-P2 moiety in which the P2-phosphido atom coordinates to the W2 metal center. The P2-W2 distance is typical for phosphido ligands coordinating to an ArN₂W (Ar = 2,6-*i*Pr₂C₆H₃) metal fragment.^{42,52,53} W1 and W2 show



distorted pseudotetrahedral geometries (considering the ligation of N1, N2, P1 and S1 for W1 and the P1-P2 bond, N3, N4 and S1 for W2). The P2-P3 bond in the uncoordinated part of the phosphorus ligand is very long (2.228(2) Å), even longer than expected for an uncoordinated P-P bond (sum of single bond covalent radii for two P = 2.22 Å).⁴⁵ The P1-P2 distance of 2.133(2) Å is only slightly shorter than typical values for coordinated P-P bonds in diphosphanylphosphido ligands (\approx 2.14-2.18 Å).^{42,52,53} The P2 and P3 atoms show pyramidal geometries with sums of the angles of $\Sigma P2 = 295.63^\circ$ and $\Sigma P3 = 308.26^\circ$, respectively.

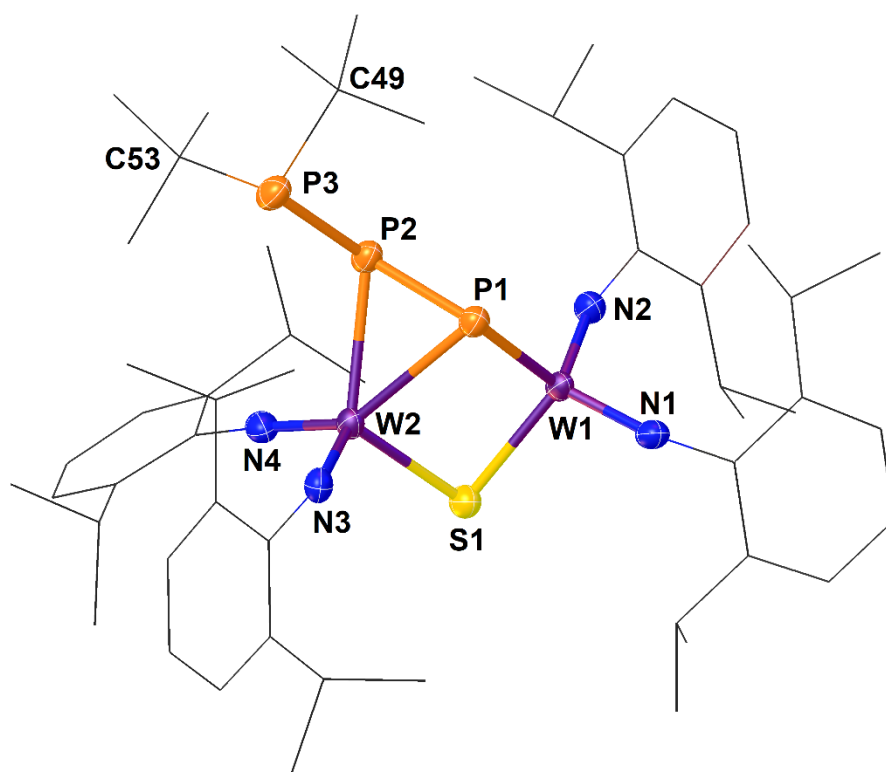


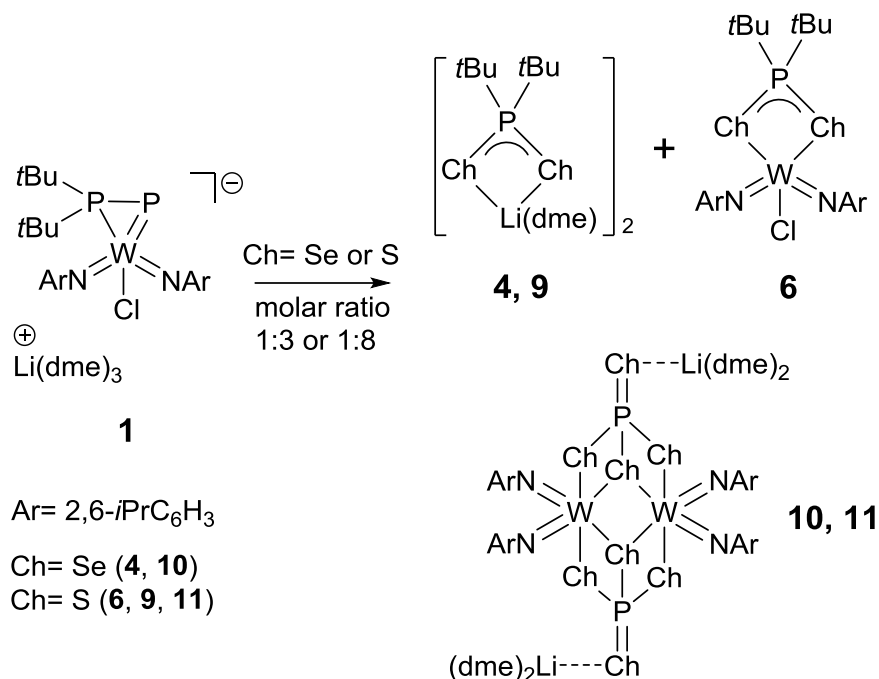
Figure 4. Molecular structure of anionic complex **8**. Ellipsoids are shown at 50% probability. H atoms are omitted for clarity. Selected bond lengths (Å) and angles ($^\circ$): P1-W2 2.714(1), P1-W1 2.364(1), P2-W2 2.483(1), P1-P2 2.133(2), P2-P3 2.228(2), P3-C49 1.890(5), P3-C53 1.898 (6), S1-W2 2.370(1), S1-W1 2.318(1), W1-P1-W2 75.81 (3), P1-W1-S1 102.62(4), P1-W2-S1 91.64(4), W1-S1-W2 83.83(4), P1-P2-P3 104.37(6), P1-P2-W2 71.58(4), W2-P2-P3 119.79(6), and P2-P1-W1 103.11(5)

Similar to that of **3**, the P1 atom exhibits a highly distorted pyramidal geometry with a very small sum of angles ($\Sigma P1 = 238.98^\circ$). The calculated Mayer bond orders for P1-W1 (1.31) and P1-W2

(0.51) are very similar to the corresponding values for **3**. Furthermore, NBO and NLMO analyses of **8** indicate delocalization of the lone pairs on the P1 and P2 atoms along the P2-P1 and P1-W1 bonds, respectively, based on the increasing π -character of these bonds.

The different behaviors of **2** and **5** in toluene and pentane can be explained by P-S bond formation being more thermodynamically favorable than P-Se bond formation. The first step of these transformations is dimerization, and this process seems to be similar for both complexes, and isolated complex **7** is an example of such an intermediate dimer. In the case of transformations involving S compounds, the strong tendency to form P-S bonds is manifested in the yield of compounds **6** and **9**, containing the $[t\text{Bu}_2\text{PS}_2]^-$ anion, followed by the elimination of a $t\text{Bu}_2\text{PS}$ moiety from transient compound **7**. Otherwise, complex **3**, the final product of the transformation of seleno-derivative **2** in toluene or pentane, is generated from the elimination of a $t\text{Bu}_2\text{P-P}$ moiety from a hypothetical dimeric complex analogous to **7**. Here, the P-Se-W structural motif is retained.

To determine the influence of excess chalcogen on the outcome of the reaction, we performed the reactions of **1** with Se or S at molar ratios of 1:3 and 1:8 (Scheme 3) under the same conditions as previously described.



Scheme 3. Reaction of **1** with excess gray selenium or sulfur.

The ³¹P NMR spectra of the reaction solutions show strong singlets for **4** (Se) or **9** (S) accompanied by a moderately intense singlet for **6** (S). Therefore, these products contain dichalcogenophosphinate fragments [*t*Bu₂PCh₂][−]. The resonances of monomeric species **2** and dimeric compounds **3**, **7** or **8** are not detected in the reaction mixtures. The work-up of the reaction solutions led to the separation of yellow crystals of [*t*Bu₂PCh₂Li(dme)]₂ (**4** and **9**) and a small amount of crystalline [W₂(DippN)₄(PCh₄)₂][Li(dme)₃]₂ (**10** and **11**) together with a polymeric, oily species that could not be characterized by ³¹P NMR spectroscopy. Complexes **10** and **11**, isolated in very low yields, are only slightly soluble in common solvents (even in THF-*d*₈), which precludes the NMR analysis of these compounds. The outcomes of these reactions indicate that an excess of chalcogen eliminates the phosphorus ligands from the tungsten centers and cleaves the P-P bonds. The X-ray structures of **10** and **11** are similar (Figure 5 and Figure S4, respectively).

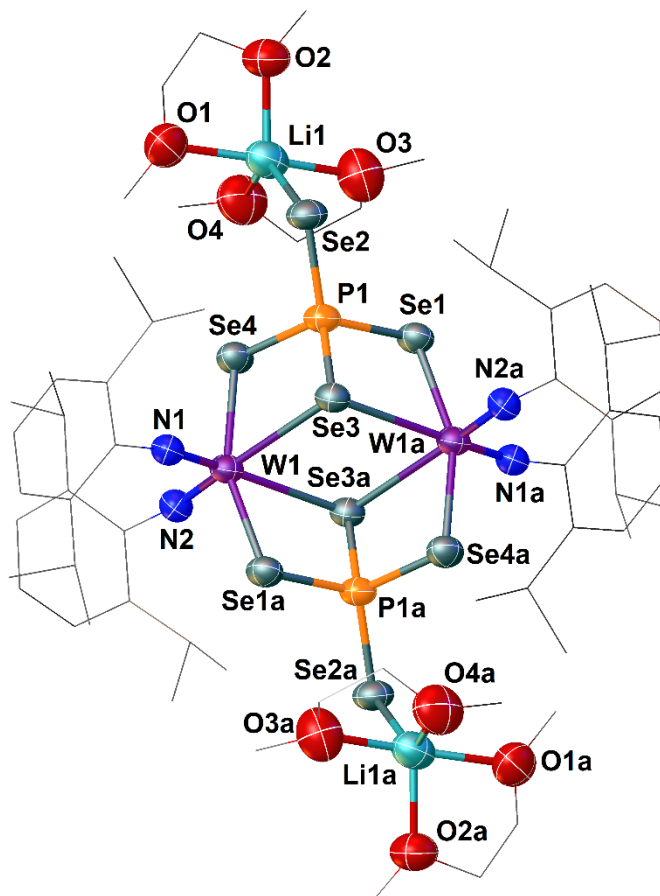


Figure 5. Molecular structure of **10**. Ellipsoids are shown at 50% probability. H atoms are omitted for clarity. Selected bond lengths (Å) and angles (°): Se1-W1a 2.5709(9), Se3-W1a 2.8680(6), Se4-W1 2.5706(9), P1-Se1 2.221(1), P1-Se2 2.132(2), P1-Se3 2.222(2), P1-Se4 2.211(1), Se2-Li1 2.948(12), P1-Se1-W1a 95.03(5), P1-Se3-W1a 87.22(4), W1a-Se3-W1 103.38(2), and Se3-W1a-Se3a 76.62(2).

The structures of **10** and **11** show that by using excess Se or S, dimeric tungsten complexes with two tetrachalcogenophosphate ligands $[\text{PCh}_4]^{3-}$ can be formed. In representative complex **10**, each tungsten atom exhibits a distorted octahedral geometry. The two metal centers are linked by Se3 and Se3a from the tetraselenophosphate ligands, forming planar four-membered rings that comprise the core of the molecule. The P atoms show tetrahedral geometries, in which the three of P-Se bonds coordinating to the tungsten atoms are essentially single bonds, while the remaining P-Se bond is significantly shorter, indicating double-bond character. Moreover, long interactions between Se2/Se2a and lithium cations are visible. Transition-metal complexes with



MOST WIEDZY Downloaded from mostwiedzy.pl

Scheme 4. Comparison of the Lewis structures of the phosphanylphosphinidene and its selenides.



Table 1. Calculated Hirshfeld charges (q) and optimized parameters for the free phosphanylphosphinidene selenides. Values in parentheses are experimental parameters for the corresponding ligands in **2** and **3**.

Compound property	<i>t</i> Bu ₂ PPSe triplet (IIa) 2	<i>t</i> Bu ₂ PPSe singlet (IIb)	<i>t</i> Bu ₂ P(Se)P triplet (IIIa) 3	<i>t</i> Bu ₂ P(Se)P singlet (IIIb)
q(P1)	0.008	0.060	-0.016	-0.145
q(P2)	0.162	0.142	0.239	0.243
q(Se)	-0.074	-0.133	-0.169	-0.065
P1-P2 (Å)	2.248 (2.248)	2.178	2.162 (2.160)	2.095
P1-Se (Å)	2.157 (2.239)	2.128	-	2.546
P2-Se (Å)	-	-	2.180 (2.202)	2.222
P2-P1-Se (°)	110.8 (104.4)	112.3	-	57.2
P1-P2-Se (°)	-	-	98.2 (94.2)	70.3

For triplet **IIa**, the highest spin densities are found on P1 and Se, which showed values of 0.822 and 0.811, respectively. The characteristic features of **IIa** are long P-P bonds and the polarization of the P-P-Se bond towards the Se atom. The P1-Se bond distance is shorter than expected for a single bond, indicating some π -interactions. The structure of triplet **IIIa** is similar to that of parent phosphanylphosphinidene **Ia**, with two singly occupied p orbitals on the P1 atom (spin density 1.573). Likewise, P1-Se bond shortening is observed in **IIa**. Singlet *t*Bu₂P2-P1-Se can be described by two resonance structures, **IIb** and **IIb'**, which show the multiple-bond character of the P1-P2 and P1-Se bonds. Interestingly, singlet **IIIb** exhibits an additional bonding interaction of P1-Se, resulting in a selenophosphirane structure. An additional characteristic feature of **IIIb** is a short P1-P2 bond polarized towards the P1 atom. The optimized structures of **Ia**, **IIb**, **IIIa** and **IIIb** are shown in Figures S52-S55. The comparison of the geometry of the *t*Bu₂P-P-Se ligand in **2** and the *t*Bu₂P(Se)-P ligand in **3** with the geometry of free selenophosphanylphosphinidenes reveals that

their geometries are similar to those of triplets **IIa** and **IIIa**, respectively (Table 1). In light of these results, complexes **2** and **3** can be seen as combinations of a triplet **IIa** or **IIIa** with a triplet transition-metal moiety. Singlet **IIb** and **IIIb** should be stabilized by late transition-metal centers (Pt) similar to what was previously observed for singlet $t\text{Bu}_2\text{P}=\text{P}$ (**Ib**).⁴⁴

3. CONCLUSIONS

Phosphanylphosphinidene complex **1** exhibits high reactivity towards chalcogens under mild conditions, and stoichiometric reactions of these compounds give the first phosphanylphosphinide chalcogenide ($t\text{Bu}_2\text{P}-\text{P}-\text{Ch}$) complexes of transition metals (**2** and **5**). The addition of the chalcogen atom to the $\text{P}=\text{W}$ bond in parent compound **1** results in the formation of a chalcogeno-phosphirane ring, and according to the X-ray crystallography and DFT studies, coordination of the $\text{P}=\text{Ch}$ double bond to a metal center can be excluded. Resulting complexes **2** and **5** are highly reactive and undergo interesting transformations in nondonor solvents, leading to new two-core tungsten complexes with chalcogenophosphinidene ($t\text{Bu}(\text{Se})\text{P}-\text{P}$), chalcogenophosphido ($t\text{Bu}_2(\text{S})\text{P}-\text{P}-\text{P}-\text{PtBu}_2$) or phosphinidene ($t\text{Bu}_2\text{P}-\text{P}-\text{P}$) ligands. The reactions of **1** with excess chalcogen led to the cleavage of the $\text{P}-\text{P}$ bond in the phosphanylphosphinidene ligand ($t\text{Bu}_2\text{P}-\text{P}$). Computational studies showed that the geometries of the $t\text{Bu}_2\text{P}-\text{P}-\text{Se}$ and $t\text{Bu}(\text{Se})\text{P}-\text{P}$ ligands in the isolated tungsten complexes are similar to the geometries of the corresponding free triplet phosphanylphosphinidene selenides.

4. EXPERIMENTAL SECTION

General information

All experiments were carried out under an argon atmosphere using Schlenk techniques. All manipulations were performed using standard vacuum, Schlenk, and glove box techniques. All

solvents were purified and dried using common methods. Solvents for NMR spectroscopy (C_6D_6 and $THF-d_8$) were purified from metallic sodium. Solids (sulfur and selenium) were kept under reduced pressure to remove traces of water. The phosphanylphosphinidene tungsten complex (2,6- $iPr_2C_6H_3N)_2(Cl)W(\eta^2-tBu_2P=P)]Li \cdot 3DME$ was synthesized following the literature method.⁴¹ NMR spectra were recorded on a Bruker Avance III HD 400 MHz spectrometer at ambient temperature (external standard TMS for 1H and ^{13}C ; 85% H_3PO_4 for ^{31}P ; Me_2Se for ^{77}Se). The chemical shift of $C(CH_3)_3$ was determined by correlation spectra due to the very weak signals in the ^{13}C NMR spectra. The NMR spectra of complex **8** were acquired at low temperature (273 K). Crystallographic analyses were performed on an STOE IPDS II diffractometer (unless stated otherwise) using MoK_{α} radiation ($\lambda = 0.71073 \text{ \AA}$) or CuK_{α} radiation ($\lambda = 1.54178 \text{ \AA}$). Elemental analyses were performed at the University of Gdańsk using a Vario El Cube CHNS apparatus.

Reaction of (2,6- $iPr_2C_6H_3N)_2(Cl)W(\eta^2-tBu_2P=P)]Li \cdot 3DME$ with gray selenium in 1:1 molar ratio (Synthesis of **2** and **3**)

A solution of (2,6- $iPr_2C_6H_3N)_2(Cl)W(\eta^2-tBu_2P=P)]Li \cdot 3DME$ (0.512 g, 0.5 mmol, 4 ml DME) was added dropwise to solid selenium (0.039 g, 0.5 mmol) at $-20^\circ C$. The reaction mixture was then warmed and stirred at ambient temperature for 24 h. The volume of the solution was reduced by half under reduced pressure, and the resulting solution was analyzed by $^{31}P\{^1H\}$ and ^{31}P NMR, which revealed that only one major product was formed. The solvent was then evaporated under reduced pressure, and the residue was partially dissolved in 10 ml of pentane. The pentane filtrate was separated from the insoluble residue, and a few red crystals of **3** (20 mg, yield 2.9%) were obtained from concentration of the pentane solution (3 ml) at ambient temperature. The pentane-insoluble residue was dissolved in 3 ml of DME and layered with 1 ml of pentane. Large orange crystals of **2** (268 mg, yield 48.4%) were obtained at $+4^\circ C$.



2: ^1H NMR (THF- d_8 , 400 MHz, δ): 0.81 (d, $^3J_{\text{HH}}=7$ Hz, 6H, $\text{HC}(\text{CH}_3)_2$), 0.83 (d, $^3J_{\text{HH}}=7$ Hz, 6H, $\text{HC}(\text{CH}_3)_2$), 0.95 (d, $^3J_{\text{PH}}=9$ Hz, 9H, $\text{C}(\text{CH}_3)_3$), 1.02 (d, overlapped, $^3J_{\text{HH}}=7$ Hz, 12H, $\text{HC}(\text{CH}_3)_2$), 1.22 (d, $^3J_{\text{PH}}=9$ Hz, 9H, $\text{C}(\text{CH}_3)_3$), 3.16 (s, 12H, CH_3O (DME)), 3.32 (s, 8H, CH_2O (DME)), 3.92 (hept, overlapped, $^3J_{\text{HH}}=7$ Hz, 4H, $\text{HC}(\text{CH}_3)_2$), 6.61 (t, $^3J_{\text{HH}}=8$ Hz, 1H, $\text{C}_{\text{Ar}}\text{H}$ -para), 6.68 (dd, $^3J_{\text{HH}}=8$ Hz, $^3J_{\text{HH}}=9$ Hz, 1H, $\text{C}_{\text{Ar}}\text{H}$ -para), 6.77 (d, overlapped, $^3J_{\text{HH}}=8$ Hz, 2H, $\text{C}_{\text{Ar}}\text{H}$ -meta), 6.79 (d, $^3J_{\text{HH}}=8$ Hz, 2H, $\text{C}_{\text{Ar}}\text{H}$ -meta); $^{31}\text{P}\{^1\text{H}\}$ NMR (THF- d_8 , 162 MHz, δ): 55.2 (d, $^1J_{\text{PP}}=263$ Hz, $t\text{Bu}_2\text{P}$), -32.2 (d, $^1J_{\text{PP}}=263$ Hz, $^1J_{\text{PW}}=58$ Hz, $^1J_{\text{PSe}}=165$ Hz, PSe); ^{13}C NMR (THF- d_8 , 100 MHz, δ): 23.05 (s, overlapped $\text{CH}(\text{CH}_3)_2$), 23.08 (s, overlapped $\text{CH}(\text{CH}_3)_2$), 23.10 (s, overlapped $\text{CH}(\text{CH}_3)_2$), 23.60 (s, $\text{CH}(\text{CH}_3)_2$), 23.64 (s, $\text{CH}(\text{CH}_3)_2$), 27.18 (s, $\text{CH}(\text{CH}_3)_2$), 27.24 (s, $\text{CH}(\text{CH}_3)_2$), 27.34 (s, $\text{CH}(\text{CH}_3)_2$), 27.40 (s, $\text{CH}(\text{CH}_3)_2$), 30.76 (dd, $^2J_{\text{CP}}=12$ Hz, $^3J_{\text{CP}}=7$ Hz, $\text{C}(\text{CH}_3)_3$), 31.68 (dd, $^2J_{\text{CP}}=13$ Hz, $^3J_{\text{CP}}=3$ Hz, $\text{C}(\text{CH}_3)_3$), 34.03 (dd, $^1J_{\text{CP}}=35$ Hz, $^2J_{\text{CP}}=10$ Hz, $\text{C}(\text{CH}_3)_3$), 35.73 (d, $^1J_{\text{CP}}=39$ Hz, $\text{C}(\text{CH}_3)_3$), 57.91 (s, CH_3O , (DME)), 71.78 (s, CH_2O (DME)), 120.03 (s, C_p), 120.64 (s, overlapped, C_m), 120.95 (s, overlapped, C_m), 123.97 (s, C_p), 139.62 (s, C_o), 145.69 (s, C_o), 152.86 (s, C_i), 155.12 (s, C_i); ^{77}Se NMR (THF- d_8 , 76 MHz, δ): -60.5 (dd, $^1J_{\text{PSe}}=165$ Hz, $^1J_{\text{WSe}}=22$ Hz, PSeW); elemental analysis calculated for $\text{C}_{44}\text{H}_{82}\text{ClLiN}_2\text{O}_6\text{P}_2\text{SeW}$ ($M=1102.27$ g/mol): C 47.94, H 7.50, N 2.54; found C 47.57, H 7.39, N 2.51.

3: ^1H NMR (C_6D_6 , 400 MHz, δ): 0.87 (d, $^3J_{\text{HH}}=7$ Hz, 6H, $\text{HC}(\text{CH}_3)_2$), 0.91 (d, overlapped, $^3J_{\text{HH}}\approx 7$ Hz, 6H, $\text{HC}(\text{CH}_3)_2$), 0.93 (d, overlapped, $^3J_{\text{PH}}=18$ Hz, 9H, $\text{C}(\text{CH}_3)_3$), 0.98 (d, $^3J_{\text{HH}}\approx 7$ Hz, 6H, $\text{HC}(\text{CH}_3)_2$), 1.01 (d, $^3J_{\text{HH}}\approx 7$ Hz, 6H, $\text{HC}(\text{CH}_3)_2$), 1.03 (d, overlapped, $^3J_{\text{PH}}=17$ Hz, 9H, $\text{C}(\text{CH}_3)_3$), 1.05 (d, overlapped, $^3J_{\text{HH}}\approx 7$ Hz, 6H, $\text{HC}(\text{CH}_3)_2$), 1.08 (d, overlapped, $^3J_{\text{HH}}\approx 7$ Hz, 6H, $\text{HC}(\text{CH}_3)_2$), 1.12 (d, $^3J_{\text{HH}}=6$ Hz, 6H, $\text{HC}(\text{CH}_3)_2$), 1.19 (d, $^3J_{\text{HH}}=7$ Hz, 6H, $\text{HC}(\text{CH}_3)_2$), 3.76 (hept, $^3J_{\text{HH}}=6$ Hz, overlapped, 4H, $\text{HC}(\text{CH}_3)_2$), 3.84 (hept, $^3J_{\text{HH}}=7$ Hz, overlapped, 4H, $\text{HC}(\text{CH}_3)_2$), 6.66-6.90 (overlapped, 12H, aromatic H); $^{31}\text{P}\{^1\text{H}\}$ NMR (C_6D_6 , 162 MHz, δ): 139.1 (d, $^1J_{\text{PP}}=451$ Hz,

$^1J_{PW} = 111$ Hz, **P**), 88.8 (d, $^1J_{PP} = 451$ Hz, $^1J_{PSe} = 370$ Hz, *t*Bu₂PSe); ^{13}C NMR (C₆D₆, 100 MHz, δ): 22.7 (s, CH(CH₃)₂), 23.3 (s, CH(CH₃)₂), 23.4 (s, CH(CH₃)₂), 23.5 (s, CH(CH₃)₂), 23.8 (s, overlapped, CH(CH₃)₂), 23.9 (s, overlapped, CH(CH₃)₂), 25.1 (s, CH(CH₃)₂), 27.0 (s, C(CH₃)₃), 28.2 (s, overlapped, C(CH₃)₃), 28.4 (s, overlapped, CH(CH₃)₂), 43.2 (broad signal, C(CH₃)₃), 43.8 (very weak broad signal, C(CH₃)₃), 121.9 (s, overlapped, C_m), 122.0 (s, overlapped, C_m), 122.2 (s, overlapped, C_m), 123.1 (s, overlapped, C_m), 124.2 (s, overlapped, C_p), 124.8 (s, C_p), 124.9 (s, C_p), 140.6 (s, overlapped, C_o), 141.2 (s, overlapped, C_o), 142.5 (s, overlapped, C_o), 147.6 (s, overlapped, C_o), 152.0 (s, overlapped, C_i), 153.7 (s, overlapped, C_i); ^{77}Se NMR (THF-d₈, 76 MHz, δ): 544.2 (s, WSeW), -281.9 (d, $^1J_{PSe} = 370$ Hz, PSeW).

Reaction of (2,6-*i*Pr₂C₆H₃N)₂(Cl)W(η^2 -*t*Bu₂P=P)]Li·3DME with sulfur in 1:1 molar ratio (synthesis of **6**, **7** and **8**)

A solution of (2,6-*i*Pr₂C₆H₃N)₂(Cl)W(η^2 -*t*Bu₂P=P)]Li·3DME (0.512 g, 0.5 mmol, 5 ml DME) was added dropwise to solid sulfur (0.016 g, 0.5 mmol) at -20°C. The reaction mixture was then warmed and stirred at ambient temperature for 24 h. The color of the solution changed from red to dark red. The volume of the solution was reduced by half under reduced pressure, and the resulting solution was analyzed by $^{31}P\{^1H\}$ and ^{31}P NMR. The solvent was then evaporated under reduced pressure, and the residue was partially extracted with petroleum ether. The petroleum ether filtrate was separated from the insoluble residue. Afterwards, the volume of the petroleum ether solution was reduced to 2 ml. Twenty milligrams of red crystals of **6** (yield 2.6%) and a few yellow crystals of **7** were obtained after storage of the solution at -30°C. The petroleum-insoluble residue was dissolved in 3 ml of toluene. A light solid precipitated, and this material was removed by filtration. The filtrate was layered with 3 ml of pentane. At first, an oil formed, and dark needle



crystals of **8** (55 mg, yield 6.9%) formed from the oil at ambient temperature. More crystals were formed after storage at lower temperature.

5: $^{31}\text{P}\{^1\text{H}\}$ NMR (C_6D_6 , 162 MHz, δ): 54.4 (d, $^1J_{\text{PP}} = 259$ Hz, $t\text{Bu}_2\text{P}$), -36.9 (d, $^1J_{\text{PP}} = 259$ Hz, **PS**).

6: ^1H NMR (C_6D_6 , 400 MHz, δ): 1.12 (d, $^3J_{\text{PH}} = 18$ Hz, 18H, $\text{C}(\text{CH}_3)_3$), 1.26 (d, $^3J_{\text{HH}} = 7$ Hz, 12H, $\text{HC}(\text{CH}_3)_2$), 1.29 (d, $^3J_{\text{HH}} = 7$ Hz, 12H, $\text{HC}(\text{CH}_3)_2$), 4.20 (hept, $^3J_{\text{HH}} = 7$ Hz, 4H, **HC**(CH_3)₂), 6.90 (t, $^3J_{\text{HH}} = 7$ Hz, 2H, $\text{C}_{\text{Ar}}\text{H}$ -para), 7.12 (d, $^3J_{\text{HH}} = 7$ Hz, 4H, $\text{C}_{\text{Ar}}\text{H}$ -meta); $^{31}\text{P}\{^1\text{H}\}$ NMR (C_6D_6 , 162 MHz, δ): 115.0 (s, $(\text{C}(\text{CH}_3)_3\text{PS}_2)$); ^{13}C NMR (C_6D_6 , 100 MHz, δ): 23.9 (s, $\text{HC}(\text{CH}_3)_2$), 24.4 (s, $\text{HC}(\text{CH}_3)_2$), 25.9 (d, $^2J_{\text{CP}} = 3$ Hz, $\text{C}(\text{CH}_3)_3$), 27.9 (s, $\text{HC}(\text{CH}_3)_2$), 42.4 (d, $^1J_{\text{CP}} = 27$ Hz, $\text{C}(\text{CH}_3)_3$), 122.2 (s, **C_m**), 126.9 (s, **C_p**), 145.2 (s, **C_o**), 151.5 (s, **C_i**).

7: ^1H NMR (C_6D_6 , 400 MHz, δ): 0.95 (d, $^3J_{\text{HH}} = 7$ Hz, 6H, $\text{HC}(\text{CH}_3)_2$), 1.10 (d, $^3J_{\text{HH}} = 7$ Hz, 6H, $\text{HC}(\text{CH}_3)_2$), 1.30 (d, overlapped, $^3J_{\text{HH}} \approx 7$ Hz, 6H, $\text{HC}(\text{CH}_3)_2$), 1.33 (d, overlapped, $^3J_{\text{HH}} \approx 7$ Hz, 24H, $\text{HC}(\text{CH}_3)_2$), 1.35 (d, overlapped, $^3J_{\text{PH}} \approx 17$ Hz, 27H, $\text{C}(\text{CH}_3)_3$), 1.45 (d, $^3J_{\text{HH}} = 7$ Hz, 6H, $\text{HC}(\text{CH}_3)_2$), 1.68 (d, $^3J_{\text{PH}} = 16$ Hz, 9H, $\text{C}(\text{CH}_3)_3$), 4.20 (hept, overlapped, $^3J_{\text{HH}} \approx 7$ Hz, 8H, **HC**(CH_3)₂), 6.82-7.13 (overlapped, 12H, aromatic **H**); $^{31}\text{P}\{^1\text{H}\}$ NMR (C_6D_6 , 162 MHz, δ): 107.7 (ddd, $^1J_{\text{PP}} = 447$ Hz, $^2J_{\text{PP}} = 80$ Hz, $^3J_{\text{PP}} = 20$ Hz, $t\text{Bu}_2\text{P}$), 74.0 (ddd, $^1J_{\text{PP}} = 431$ Hz, $^2J_{\text{PP}} = 155$ Hz, $^3J_{\text{PP}} = 20$ Hz, $t\text{Bu}_2\text{P}$); -46.4 (ddd, $^1J_{\text{PP}} = 431$ Hz, $^2J_{\text{PP}} = 264$ Hz, $^2J_{\text{PP}} = 80$ Hz, $^1J_{\text{PW}} = 50$ Hz, **P**), -190.5 (ddd, $^1J_{\text{PP}} = 447$ Hz, $^2J_{\text{PP}} = 264$ Hz, $^2J_{\text{PP}} = 155$ Hz, $^1J_{\text{PW}} = 32$ Hz, **P**); ^{13}C NMR (C_6D_6 , 100 MHz, δ): 22.7 (s, $\text{HC}(\text{CH}_3)_2$), 23.2 (s, $\text{HC}(\text{CH}_3)_2$), 23.7 (s, $\text{HC}(\text{CH}_3)_2$), 24.3 (s, $\text{HC}(\text{CH}_3)_2$), 25.4 (s, $\text{HC}(\text{CH}_3)_2$), 26.6 (d, $^2J_{\text{CP}} = 8$ Hz, $\text{C}(\text{CH}_3)_3$), 27.6 (s, overlapped, $\text{HC}(\text{CH}_3)_2$), 27.7 (s, overlapped, $\text{HC}(\text{CH}_3)_2$), 28.2 (s, overlapped, $\text{HC}(\text{CH}_3)_2$), 28.3 (d, $^2J_{\text{CP}} = 5$ Hz, $\text{C}(\text{CH}_3)_3$), 30.4 (broad, $\text{C}(\text{CH}_3)_3$), 31.6 (broad, $\text{C}(\text{CH}_3)_3$), 35.5 (very weak signal, $\text{C}(\text{CH}_3)_3$), 38.6 (very weak signal, $\text{C}(\text{CH}_3)_3$), 42.2 (very weak signal, $\text{C}(\text{CH}_3)_3$), 44.8 (broad, very weak signal, $\text{C}(\text{CH}_3)_3$), 122.38 (s, overlapped, **C_m**),

122.44 (s, overlapped, C_m), 122.62 (s, overlapped, C_m), 124.21 (s, overlapped, C_m), 126.2 (s, overlapped, C_p), 126.3 (s, overlapped, C_p), 143.6 (s, overlapped, C_o), 145.4 (s, overlapped, C_o), 145.9 (s, overlapped, C_o), 142.5 (s, overlapped, C_o), 147.6 (s, overlapped, C_o), 152.9 (s, weak, C_i), 154.6 (s, weak, C_i)

8: ¹H NMR (THF-d₈, 400 MHz, 273K, δ): 0.74 (d, ³J_{HH} = 7 Hz, 6H, HC(CH₃)₂), 0.79 (d, ³J_{HH} = 7 Hz, 6H, HC(CH₃)₂), 1.05 (d, ³J_{HH} = 7 Hz, 6H, HC(CH₃)₂), 1.12 (d, ³J_{HH} = 7 Hz, overlapped, 24H, HC(CH₃)₂), 1.17 (d, ³J_{HH} = 7 Hz, 6H, HC(CH₃)₂), 1.41 (d, ³J_{PH} = 10 Hz, 9H, C(CH₃)₃), 1.64 (d, ³J_{PH} = 10 Hz, 9H, C(CH₃)₃), 2.34 (s, 3H, CH₃-C₆H₅ (toluene)), 3.30 (s, 12H, CH₃O (diglyme)), 3.46 (m, 8H, CH₂ (diglyme)), 3.55 (m, 8H, CH₂ (diglyme)), 3.66 (hept, ³J_{HH} ≈ 7 Hz, overlapped, 2H, HC(CH₃)₂), 3.81 (hept, ³J_{HH} ≈ 7 Hz, overlapped, 2H, HC(CH₃)₂), 4.00 (hept, ³J_{HH} ≈ 7 Hz, overlapped, 2H, HC(CH₃)₂), 4.09 (hept, ³J_{HH} ≈ 7 Hz, overlapped, 2H, HC(CH₃)₂), 6.62 (t, ³J_{HH} = 7 Hz, 1H, C_{Ar}-H), 6.73-7.00 (overlapped, 11H, C_{Ar}-H), 7.15 (m, 3H, C_{Ar}-H, toluene), 7.23 (m, 2H, C_{Ar}-H, toluene); ³¹P {¹H} NMR (THF-d₈, 162 MHz, δ): 388.7 (dd, ¹J_{PP} = 385 Hz, ²J_{PP} = 36 Hz, P), 134.1 (dd, ¹J_{PP} = 385 Hz, ¹J_{PP} = 276 Hz, ¹J_{PW} = 87 Hz, P), 77.8 (dd, ¹J_{PP} = 276 Hz, ²J_{PP} = 36 Hz *t*Bu₂P); ¹³C NMR (THF-d₈, 100 MHz, 273K, δ): 20.6 (s, CH₃C₆H₅, toluene), 22.8 (s, CH(CH₃)₂), 23.1 (s, CH(CH₃)₂), 23.2 (s, CH(CH₃)₂), 23.3 (s, overlapped, CH(CH₃)₂), 23.4 (s, overlapped, CH(CH₃)₂), 23.5 (s, CH(CH₃)₂), 27.4 (s, overlapped, CH(CH₃)₂), 27.5 (s, overlapped, CH(CH₃)₂), 27.6 (s, overlapped, CH(CH₃)₂), 27.7 (s, overlapped, CH(CH₃)₂), 27.8 (s, overlapped, CH(CH₃)₂), 31.3 (d, overlapped, ²J_{CP} = 14 Hz, C(CH₃)₃), 32.0 (d, overlapped, ³J_{CP} = 14 Hz, C(CH₃)₃), 36.0 (d, overlapped, ¹J_{CP} = 40 Hz, C(CH₃)₃), 58.0 (s, CH₃, diglyme), 70.3 (s, CH₂, diglyme), 71.8 (s, CH₂, diglyme), 119.4 (s, overlapped, C_m), 120.5 (s, overlapped, C_m), 120.8 (s, overlapped, C_m), 121.3 (s, overlapped, C_m), 122.0 (s, overlapped, C_p), 123.2 (s, overlapped, C_p), 125.1 (s, C_p, toluene), 128.0 (s, C_m, toluene), 128.7 (s, C_o, toluene), 137.5 (s, C_i, toluene), 139.4 (s, overlapped, C_o),

139.5 (s, overlapped, C_o), 141.4 (s, overlapped, C_o), 145.6 (s, overlapped, C_o), 154.0 (s, C_i), 155.2 (s, C_i), 155.3 (s, C_i), 155.4 (s, C_i); elemental analysis calculated for C₇₅H₁₂₂LiN₄O₆P₃SW₂ (M= 1675.40 g/mol): C 53.77, H 7.34, N 3.34, S 1.92; found C 52.90, H 7.23, N 3.34, S 1.91. The value found for carbon is too low due to the formation of tungsten carbide.

Reaction of (2,6-*i*Pr₂C₆H₃N)₂(Cl)W(η²-*t*Bu₂P=P)]Li·3DME with gray selenium in the molar ratio 1:8 (synthesis of **4** and **10**)

A solution of (2,6-*i*Pr₂C₆H₃N)₂(Cl)W(η²-*t*Bu₂P=P)]Li·3DME (0.512 g, 0.5 mmol, 5 ml of DME) was added dropwise to solid selenium (0.316 g, 4 mmol) at -20°C. The reaction mixture was then warmed and stirred at ambient temperature for 24 h. The volume of the solution was reduced by half under reduced pressure, and the resulting solution was analyzed by ³¹P{¹H} and ³¹P NMR. The solvent was then evaporated under reduced pressure, and the residue was partially dissolved in pentane. The pentane filtrate was separated from the insoluble residue, and then the volume of the solution was reduced to 3 ml. A small number of yellowish crystals of **4** (15 mg, yield 7.5%) were obtained after 24 h at ambient temperature. The pentane-insoluble residue was dissolved in 4 ml of toluene. A small number of thin needle-shaped dark crystals of **10** formed at ambient temperature. Further attempts to obtain more crystalline product failed and resulted in the formation of oils that were insoluble in all accessible solvents.

4: ¹H NMR (C₆D₆, 400 MHz, δ): 1.70 (d, ³J_{PH}=16 Hz, 18H, C(CH₃)₃), 2.66 (s, 4H, OCH₂ (DME)), 3.04 (s, 6H, OCH₃ (DME)); ³¹P{¹H} NMR (C₆D₆, 162 MHz, δ): 88.5 (s, ¹J_{PSe}= 546 Hz, (C(CH₃)₃PSe₂); ¹³C NMR (C₆D₆, 100 MHz, δ): 28.2 (d, ²J_{CP}= 4 Hz, C(CH₃)₃), 40.1 (d, ¹J_{CP}= 25 Hz, C(CH₃)₃), 58.9 (s, CH₃O, (DME)), 69.4 (s, CH₂O, (DME)) ⁷⁷Se NMR (THF-d₈, 76 MHz, δ):



- 200.5 (d, $^1J_{\text{PSe}} = 546$ Hz, PSeLi); elemental analysis calculated for $\text{C}_{12}\text{H}_{28}\text{LiO}_2\text{PSe}_2$ ($M = 400.18$ g/mol): C 36.02, H 7.05; found C 35.53, H 6.77.

Reaction of $(2,6\text{-}i\text{Pr}_2\text{C}_6\text{H}_3\text{N})_2(\text{Cl})\text{W}(\eta^2\text{-}t\text{Bu}_2\text{P}=\text{P})\text{Li}\cdot 3\text{DME}$ with sulfur in 1:3 molar ratio
(Synthesis of **9** and **11**)

A solution of $(2,6\text{-}i\text{Pr}_2\text{C}_6\text{H}_3\text{N})_2(\text{Cl})\text{W}(\eta^2\text{-}t\text{Bu}_2\text{P}=\text{P})\text{Li}\cdot 3\text{DME}$ (0.512 g, 0.5 mmol, 5 ml of DME) was added dropwise to solid sulfur (0.048 g, 1.5 mmol) at -20°C . The reaction mixture was then warmed and stirred at ambient temperature for 24 h. The volume of solution was reduced by half under reduced pressure, and the resulting solution was analyzed by $^{31}\text{P}\{^1\text{H}\}$ and ^{31}P NMR. The solvent was then evaporated under reduced pressure, and the residue was partially dissolved in pentane. Then, the volume of the solution was reduced to 3 ml. A small number of yellowish crystals of **9** (17 mg, yield 11%) were obtained after 24 h at ambient temperature. The pentane-insoluble residue was dissolved in 4 ml of toluene. A small number of thin needle-shaped dark crystals of **11** formed at $+4^\circ\text{C}$. Further attempts to obtain more crystalline product failed and resulted in the formation of an oil that was insoluble in all accessible solvents.

9: ^1H NMR (C_6D_6 , 400 MHz, δ): 1.67 (d, $^3J_{\text{PH}} = 16$ Hz, 18H, $\text{C}(\text{CH}_3)_3$), 2.66 (s, 4H, OCH_2 (DME)), 3.04 (s, 6H, OCH_3 (DME)); $^{31}\text{P}\{^1\text{H}\}$ NMR (C_6D_6 , 162 MHz, δ): 110.2 (s, $(\text{C}(\text{CH}_3)_3\text{PS}_2)$); ^{13}C NMR (C_6D_6 , 100 MHz, δ): 27.9 (d, $^2J_{\text{CP}} = 3$ Hz, $\text{C}(\text{CH}_3)_3$), 41.1 (d, $^1J_{\text{CP}} = 40$ Hz, $\text{C}(\text{CH}_3)_3$), 58.8 (s, CH_3O (DME)), 69.5 (s, CH_2O (DME)).

5. CONFLICTS OF INTERESTS

There are no conflicts to declare.

6. ACKNOWLEDGMENTS

A.O. and J.P. thank the National Science Centre, Poland (Grant 2017/25/N/ST5/00766) for financial support. The authors thank TASK Computational Center for access to computational resources.

REFERENCES

- (1) Liu, L.; Ruiz, D. A.; Munz, D.; Bertrand, G. A Singlet Phosphinidene Stable at Room Temperature. *Chem* **2016**, *1* (1), 147–153 DOI: 10.1016/j.chempr.2016.04.001.
- (2) Aktaş, H.; Chris Slootweg, J.; Lammertsma, K. Nucleophilic Phosphinidene Complexes: Access and Applicability. *Angew. Chemie - Int. Ed.* **2010**, *49* (12), 2102–2113 DOI: 10.1002/anie.200905689.
- (3) Lammertsma, K.; Vlaar, M. J. M. Carbene-like Chemistry of Phosphinidene Complexes - Reactions, Applications, and Mechanistic Insights. *European J. Org. Chem.* **2002**, 1127–1138 DOI: 10.1002/1099-0690(200204)2002:7<1127::AID-EJOC1127>3.0.CO;2-X.
- (4) Cowley, A. H. Terminal Phosphinidene and Heavier Congeneric Complexes. The Quest Is Over. *Acc. Chem. Res.* **1997**, *30* (11), 445–451 DOI: 10.1021/ar970055e.
- (5) Mathey, F. The Development of a Carbene-like Chemistry with Terminal Phosphinidene Complexes. *Angew. Chemie Int. Ed. English* **1987**, *26* (4), 275–286 DOI: 10.1002/anie.198702753.
- (6) Mathey, F.; Huy, N. H. T.; Marinetti, A. Electrophilic Terminal-Phosphinidene Complexes: Versatile Phosphorus Analogues of Singlet Carbenes. *Helv. Chim. Acta* **2001**, *84* (10), 2938–2957 DOI: 10.1002/1522-2675(20011017)84:10<2938::AID-HLCA2938>3.0.CO;2-P.

- (7) Olkowska-Oetzel, J.; Pikies, J. Review: Chemistry of the Phosphinophosphinidene Chemistry of the Phosphinophosphinidene $t\text{Bu}_2\text{P-P}$, a Novel π -Electron Ligand. *Appl. Organomet. Chem.* **2003**, *17* (1), 28–35 DOI: 10.1002/aoc.387.
- (8) Hansmann, M. M.; Jazzar, R.; Bertrand, G. Singlet (Phosphino)Phosphinidenes Are Electrophilic. *J. Am. Chem. Soc.* **2016**, *138* (27), 8356–8359 DOI: 10.1021/jacs.6b04232.
- (9) Back, O.; Henry-Ellinger, M.; Martin, C. D.; Martin, D.; Bertrand, G. ^{31}P NMR Chemical Shifts of Carbene-Phosphinidene Adducts as an Indicator of the π -Accepting Properties of Carbenes. *Angew. Chemie Int. Ed.* **2013**, *52* (10), 2939–2943 DOI: 10.1002/anie.201209109.
- (10) Shah, S.; Protasiewicz, J. D. ‘Phospha-Variations’ on the Themes of Staudinger and Wittig: Phosphorus Analogs of Wittig Reagents. *Coord. Chem. Rev.* **2000**, *210* (1), 181–201 DOI: 10.1016/S0010-8545(00)00311-8.
- (11) Fritz, G.; Vaahs, T.; Fleischer, H.; Matern, E. $t\text{Bu}_2\text{P-P}=\text{PBr}t\text{Bu}_2\cdot\text{LiBr}$ and the Formation of $t\text{Bu}_2\text{P-P}$. *Angew. Chemie Int. Ed. English* **1989**, *28* (3), 315–316 DOI: 10.1002/anie.198903151.
- (12) Krautscheid, H.; Matern, E.; Kovacs, I.; Fritz, G.; Pikies, J. Komplexchemie P-Reicher Phosphane Und Silylphosphane. XIV. Phosphinophosphiniden $t\text{Bu}_2\text{P-P}$ Als Ligand in Den Pt-Komplexen $[\eta^2\text{-}\{t\text{Bu}_2\text{P-P}\}\text{Pt}(\text{PPh}_3)_2]$ Und $[\eta^2\text{-}\{t\text{Bu}_2\text{P-P}\}\text{Pt}(\text{PEtPh}_2)_2]$. *Zeitschrift für Anorg. und Allg. Chemie* **1997**, *623* (12), 1917–1924 DOI: 10.1002/zaac.19976231216.
- (13) Kilgore, U. J.; Fan, H.; Pink, M.; Urnezis, E.; Protasiewicz, J. D.; Mindiola, D. J. Phosphinidene Group-Transfer with a Phospha-Wittig Reagent: A New Entry to Transition



Metal Phosphorus Multiple Bonds. *Chem. Commun.* **2009**, No. 30, 4521 DOI: 10.1039/b910410k.

- (14) Graham, C. M. E.; Pritchard, T. E.; Boyle, P. D.; Valjus, J.; Tuononen, H. M.; Ragogna, P. J. Trapping Rare and Elusive Phosphinidene Chalcogenides. *Angew. Chemie - Int. Ed.* **2017**, *56* (22), 6236–6240 DOI: 10.1002/anie.201611196.
- (15) Graham, C. M. E.; Valjus, J.; Pritchard, T. E.; Boyle, P. D.; Tuononen, H. M.; Ragogna, P. J. Phosphorus-Chalcogen Ring Expansion and Metal Coordination. *Inorg. Chem.* **2017**, *56* (21), 13500–13509 DOI: 10.1021/acs.inorgchem.7b02217.
- (16) Gaspar, P. P.; Qian, H.; Beatty, A. M.; André D'Avignon, D.; Kao, J. L. F.; Watt, J. C.; Rath, N. P. 2,6-Dimethoxyphenylphosphirane Oxide and Sulfide and Their Thermolysis to Phosphinidene Chalcogenides - Kinetic and Mechanistic Studies. *Tetrahedron* **2000**, *56* (1), 105–119 DOI: 10.1016/S0040-4020(99)00779-6.
- (17) Cummins, C. C. Reductive Cleavage and Related Reactions Leading to Molybdenum–element Multiple Bonds: New Pathways Offered by Three-Coordinate Molybdenum(III). *Chem. Commun.* **1998**, 7 (17), 1777–1786 DOI: 10.1039/a802402b.
- (18) Balázs, G.; Green, J. C.; Scheer, M. Terminally Coordinated AsS and PS Ligands. *Chem. - A Eur. J.* **2006**, *12* (33), 8603–8608 DOI: 10.1002/chem.200600975.
- (19) Weber, L.; Meine, G.; Niederpruem, N.; Boese, R. Transition-Metal-Substituted Diphosphenes. 10. Reaction of the Diphosphenyl Complex $(\eta^5\text{-C}_5\text{Me}_5)(\text{CO})_2\text{FeP=PAr}$ (Ar = 2,4,6-*t*-Bu₃C₆H₂) with Sulfur and Selenium. Preparation and x-Ray Structure Analysis of the First Phosphinidene(Thioxo)Phosphoranyl Complex. *Organometallics* **1987**, *6* (9),

1989–1991 DOI: 10.1021/om00152a028.

- (20) Reisacher, H. U.; McNamara, W. F.; Duesler, E. N.; Paine, R. T. Reactions of Molybdenum and Tungsten Phosphenium Complexes with Sulfur and Selenium. *Organometallics* **1997**, *16* (3), 449–455 DOI: 10.1021/om9605490.
- (21) Malisch, W.; Grün, K.; Hirth, U.-A.; Noltemeyer, M. Phosphenium-Übergangsmetallkomplexe XXVIII. PH-Funktiionalisierte Phosphametallacyclen $C_5R_5(OC)_2W-PH(t-Bu)-X$ ($R = H, Me$; $X = S, Se, Te$) Mit Dreiringstruktur. *J. Organomet. Chem.* **1996**, *513* (1–2), 31–36 DOI: 10.1016/0022-328X(95)05875-P.
- (22) Lorenz, I. -P; Mürschel, P.; Pohl, W.; Polborn, K. Mono- Und Diferriophosphane Und -thioxophosphorane. *Chem. Ber.* **1995**, *128* (4), 413–416 DOI: 10.1002/cber.19951280413.
- (23) Hitchcock, P. B.; Johnson, J. A.; Lemos, M. A. N. D. A.; Meidine, M. F.; Nixon, J. F.; Pombeiro, A. J. L. Novel Synthesis of a Phosphinidene Oxide- κP ($RP=O$, $R = Bu^tCH_2-$) Complex of Rhenium(I) from a Phosphaalkyne Precursor. Crystal and Molecular Structure of $[ReCl(Ph_2PCH_2CH_2PPh_2)_2\{P(O)CH_2Bu^t\}]$. *J. Chem. Soc., Chem. Commun.* **1992**, No. 8, 645–646 DOI: 10.1039/C39920000645.
- (24) Alonso, M.; García, M. E.; Ruiz, M. A.; Hamidov, H.; Jeffery, J. C. Chemistry of the Phosphinidene Oxide Ligand. *J. Am. Chem. Soc.* **2004**, *126* (42), 13610–13611 DOI: 10.1021/ja045487g.
- (25) Alonso, M.; Alvarez, M. A.; García, M. E.; García-Vivó, D.; Ruiz, M. A. Chemistry of the Oxophosphinidene Ligand. 1. Electronic Structure of the Anionic Complexes $[MCp\{P(O)R^*\}(CO)_2]-(M = Mo, W; R^* = 2,4,6-C_6H_2^tBu_3)$ and Their Reactions with H^+



and C-Based Electrophiles. *Inorg. Chem.* **2010**, *49* (19), 8962–8976 DOI: 10.1021/ic101261f.

- (26) Alonso, M.; Alvarez, M. A.; García, M. E.; Ruiz, M. A.; Hamidov, H.; Jeffery, J. C. Oxidation Reactions of the Phosphinidene Oxide Ligand. *J. Am. Chem. Soc.* **2005**, *127* (43), 15012–15013 DOI: 10.1021/ja054941t.
- (27) Alonso, M.; Alvarez, M. A.; García, M. E.; García-Vivó, D.; Ruiz, M. A. Nucleophilic Behaviour of Dioxo- and Thiooxophosphorane Complexes $[\text{MoCp}(\text{CO})_2\{\text{E,P-EP}(\text{O})(2,4,6\text{-C}_6\text{H}_2^t\text{Bu}_3)\}](\text{E} = \text{O}, \text{S})$. *Dalt. Trans.* **2014**, *43* (42), 16074–16083 DOI: 10.1039/c4dt01942c.
- (28) García, M. E.; García-Vivó, D.; Ramos, A.; Ruiz, M. A. Phosphinidene-Bridged Binuclear Complexes. *Coord. Chem. Rev.* **2017**, *330*, 1–36 DOI: 10.1016/j.ccr.2016.09.008.
- (29) Schmitt, G.; Ullrich, D.; Wolmershäuser, G.; Regitz, M.; Scherer, O. J. $t\text{BuC}\equiv\text{P}$ Als Edukt Für Die Bildung Eines Rhenium-Zweikernkomplexes Mit Einem Verbrückenden, Chiralen Phosphinidenoxid-Liganden. *Zeitschrift für Anorg. und Allg. Chemie* **1999**, *625* (5), 702–704 DOI: 10.1002/(SICI)1521-3749(199905)625:5<702::AID-ZAAC702>3.0.CO;2-C.
- (30) Hirth, U. A.; Malisch, W.; Käß, H. Phosphenium-Übergangsmetallkomplexe. XXI. Schwefel- Und Selenaddition an Die Metall-Phosphor-Doppelbindung Der Zweikernigen Phosphinidenkomplexe $\text{Cp}(\text{CO})_2\text{M}=\text{PMes}[\text{M}(\text{CO})_3\text{Cp}]$ ($\text{M} = \text{Mo}, \text{W}$). *J. Organomet. Chem.* **1992**, *439* (1), 20–24 DOI: 10.1016/0022-328X(92)80062-3.
- (31) Lv, Y.; Kefalidis, C. E.; Zhou, J.; Maron, L.; Leng, X.; Chen, Y. Versatile Reactivity of a Four-Coordinate Scandium Phosphinidene Complex: Reduction, Addition, and CO

Activation Reactions. *J. Am. Chem. Soc.* **2013**, *135* (39), 14784–14796 DOI: 10.1021/ja406413d.

- (32) Kourkine, I.; Glueck, D. Synthesis and Reactivity of a Dimeric Platinum Phosphinidene Complex. *Inorg. Chem.* **1997**, *36* (9), 5160–5164 DOI: 10.1021/ic970730g.
- (33) Alvarez, C. M.; Alvarez, M. A.; García, M. E.; Ramos, A.; Ruiz, M. A.; Lanfranchi, M.; Tiripicchio, A. A Triply Bonded Dimolybdenum Hydride Complex with Acid, Base and Radical Activity. *Organometallics* **2005**, *24* (1), 7–9 DOI: 10.1021/om0491948.
- (34) Alvarez, M. A.; García, M. E.; González, R.; Ruiz, M. a. Reactions of the Phosphinidene-Bridged Complexes $[\text{Fe}_2(\eta^5\text{-C}_5\text{H}_5)_2(\mu\text{-PR})(\mu\text{-CO})(\text{CO})_2]$ (R = Cy, Ph) with Electrophiles Based on p-Block Elements. *Dalt. Trans.* **2012**, *41* (48), 9005–9018 DOI: 10.1039/c2dt31506h.
- (35) Alvarez, M. A.; García, M. E.; González, R.; Ramos, A.; Ruiz, M. A. Chemical and Structural Effects of Bulkness on Bent-Phosphinidene Bridges: Synthesis and Reactivity of the Diiron Complex $[\text{Fe}_2\text{Cp}_2\{\mu\text{-P}(2,4,6\text{-C}_6\text{H}_2\text{tBu}_3)\}(\mu\text{-CO})(\text{CO})_2]$. *Organometallics* **2010**, *29* (8), 1875–1878 DOI: 10.1021/om100137d.
- (36) Alvarez, B.; Alvarez, M. A.; Amor, I.; García, M. E.; García-Vivó, D.; Suárez, J.; Ruiz, M. A. Dimolybdenum Cyclopentadienyl Complexes with Bridging Chalcogenophosphinidene Ligands. *Inorg. Chem.* **2012**, *51* (14), 7810–7824 DOI: 10.1021/ic300869z.
- (37) Alvarez, B.; Angeles Alvarez, M.; Amor, I.; García, M. E.; Ruiz, M. A. A Thiophosphinidene Complex as a Vehicle in Phosphinidene Transmetalation: Easy Formation and Cleavage of a P-S Bond. *Inorg. Chem.* **2011**, *50* (21), 10561–10563 DOI:

10.1021/ic202058h.

- (38) Alvarez, B.; Alvarez, M. A.; García, M. E.; Ruiz, M. A. P-S Bond Cleavage in Reactions of Thiophosphinidene-Bridged Dimolybdenum Complexes with $[\text{Co}_2(\text{CO})_8]$ to Give Phosphinidene-Bridged Heterometallic Derivatives. *Dalt. Trans.* **2016**, 45 (5), 1937–1952 DOI: 10.1039/c5dt01450f.
- (39) Ehlers, A. W.; Baerends, E. J.; Lammertsma, K. Nucleophilic or Electrophilic Phosphinidene Complexes $\text{ML}_n=\text{PH}$; What Makes the Difference? *J. Am. Chem. Soc.* **2002**, 124 (11), 2831–2838 DOI: 10.1021/ja017445n.
- (40) Graham, T. W.; Udachin, K. A.; Carty, A. J. Synthesis of σ - π -Phosphinidene Sulfide Complexes $[\text{Mn}_2(\text{CO})_n(\mu\text{-}\eta^1, \eta^2\text{-P}(\text{NR}_2)\text{S})]$ ($N=8,9$) via Direct Sulfuration of Electrophilic μ -Phosphinidenes and Photochemical Transformation to a Trigonal Prismatic $\text{Mn}_2\text{P}_2\text{S}_2$ Cluster. *Inorganica Chim. Acta* **2007**, 360 (4), 1376–1379 DOI: 10.1016/j.ica.2006.02.022.
- (41) Grubba, R.; Baranowska, K.; Chojnacki, J.; Pikies, J. Access to Side-On Bonded Tungsten Phosphanylphosphinidene Complexes. *Eur. J. Inorg. Chem.* **2012**, 2012 (20), 3263–3265 DOI: 10.1002/ejic.201200456.
- (42) Grubba, R.; Ordyszewska, A.; Kaniewska, K.; Ponikiewski, Ł.; Chojnacki, J.; Gudat, D.; Pikies, J. Reactivity of Phosphanylphosphinidene Complex of Tungsten(VI) toward Phosphines: A New Method of Synthesis of Catena -Polyphosphorus Ligands. *Inorg. Chem.* **2015**, 54 (17), 8380–8387 DOI: 10.1021/acs.inorgchem.5b01063.
- (43) Grubba, R.; Ordyszewska, A.; Ponikiewski, Ł.; Gudat, D.; Pikies, J. An Investigation on the Chemistry of the $\text{R}_2\text{P}=\text{P}$ Ligand: Reactions of a Phosphanylphosphinidene Complex of

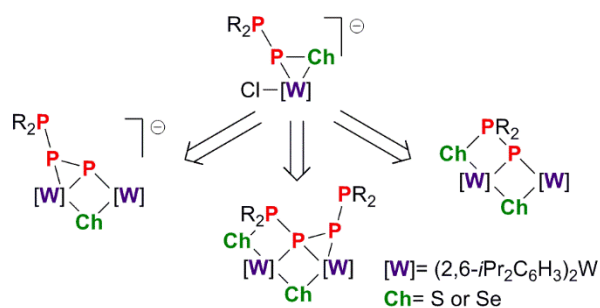
Tungsten(VI) with Electrophilic Reagents. *Dalt. Trans.* **2016**, 45 (5), 2172–2179 DOI: 10.1039/C5DT03085D.

- (44) Zauliczny, M.; Ordyszewska, A.; Pikies, J.; Grubba, R. Bonding in Phosphanylphosphinidene Complexes of Transition Metals and Their Correlation with Structures, ^{31}P NMR Spectra, and Reactivities. *Eur. J. Inorg. Chem.* **2018**, 2018 (26), 3131–3141 DOI: 10.1002/ejic.201800270.
- (45) Pyykkö, P.; Atsumi, M. Molecular Single-Bond Covalent Radii for Elements 1-118. *Chem. - A Eur. J.* **2009**, 15 (1), 186–197 DOI: 10.1002/chem.200800987.
- (46) Alper, H.; Petrignani, J. F.; Einstein, F. W. B.; Willis, A. C. Binuclear Phosphinothioylidene Complexes. *Organometallics* **1983**, 2 (10), 1422–1426 DOI: 10.1021/om50004a030.
- (47) Lindner, E.; Auch, K.; Hiller, W.; Fawzi, R. Methyl(Thioxo)Phosphane: Generation and Trapping Reaction with $\text{Mn}_2(\text{CO})_{10}$. *Angew. Chemie Int. Ed. English* **1984**, 23 (4), 320–320 DOI: 10.1002/anie.198403201.
- (48) Hussong, R.; Heydt, H.; Maas, G.; Regitz, M. Phosphorverbindungen Ungewöhnlicher Koordination, 17¹⁾ Über Die Abfangreaktion von Phenylthioxophosphan Mit Hexacarbonylbis(Cyclopentadienyl)Dimolybdän. *Chem. Ber.* **1987**, 120 (7), 1263–1267 DOI: 10.1002/cber.19871200727.
- (49) Pyykkö, P.; Atsumi, M. Molecular Double-Bond Covalent Radii for Elements Li-E112. *Chem. - A Eur. J.* **2009**, 15 (46), 12770–12779 DOI: 10.1002/chem.200901472.
- (50) Surgenor, B. a; Chalmers, B. a; Athukorala Arachchige, K. S.; Slawin, A. M. Z.; Woollins,

- J. D.; Bühl, M.; Kilian, P. Reactivity Profile of a Peri-Substitution-Stabilized Phosphanylidene-Phosphorane: Synthetic, Structural, and Computational Studies. *Inorg. Chem.* **2014**, 53 (13), 6856–6866 DOI: 10.1021/ic500697m.
- (51) Grubba, R.; Zauliczny, M.; Ponikiewski, Ł.; Pikies, J. The Reactivity of 1,1-Dichloro-2,2-Di-*Tert*-Butyldiphosphane towards Lithiated Metal Carbonyls: A New Entry to Phosphanylphosphinidene Dimers. *Dalt. Trans.* **2016**, 45 (12) DOI: 10.1039/c5dt04983k.
- (52) Grubba, R.; Wiśniewska, A.; Ponikiewski, Ł.; Caporali, M.; Peruzzini, M.; Pikies, J. Reactivity of Diimido Complexes of Molybdenum and Tungsten towards Lithium Derivatives of Diphosphanes and Triphosphanes. *Eur. J. Inorg. Chem.* **2014**, No. 10, 1811–1817 DOI: 10.1002/ejic.201301302.
- (53) Wiśniewska, A.; Grubba, R.; Ponikiewski, Ł.; Zauliczny, M.; Pikies, J. The New Diphosphanylphosphido Complexes of Tungsten(VI) and Molybdenum(VI). Their Synthesis, Structures and Properties. *Dalt. Trans.* **2018**, 47 (30), 10213–10222 DOI: 10.1039/C8DT01977K.
- (54) Chondroudis, K.; Kanatzidis, M. G.; Sayettat, J.; Jobic, S.; Brec, R. Palladium Chemistry in Molten Alkali Metal Polychalcophosphate Fluxes. Synthesis and Characterization of $K_4Pd(PS_4)_2$, $Cs_4Pd(PSe_4)_2$, $Cs_{10}Pd(PSe_4)_4$, $KPdPS_4$, $K_2PdP_2S_6$, and $Cs_2PdP_2Se_6$. *Inorg. Chem.* **1997**, 36 (25), 5859–5868 DOI: 10.1021/ic970593n.
- (55) Chondroudis, K.; Kanatzidis, M. G. $[M_4(Se_2)_2(PSe_4)_4]^{8-}$: A Novel, Tetranuclear, Cluster Anion with a Stellane-like Core. *Chem. Commun.* **1997**, 4 (4), 401–402 DOI: 10.1039/a607549e.

- (56) Chondroudis, K.; Kanatzidis, M. G. $[\text{Ce}(\text{PSe}_4)_4]^{9-}$: A Highly Anionic Ce^{3+} Selenophosphate Coordination Complex. *Inorg. Chem. Commun.* **1998**, 1 (2), 55–57 DOI: 10.1016/S1387-7003(98)00011-2.

For Table of Contents Only



Synopsis:

The syntheses of the first phosphanylphosphinidene chalcogenide ($t\text{Bu}_2\text{P-P-Ch}$) complexes of transition metals are presented. The resulting complexes are highly reactive and undergo transformations in nondonor solvents leading to new dinuclear tungsten complexes with chalcogenophosphinidene ($t\text{Bu}(\text{Se})\text{P-P}$), chalcogenophosphido ($t\text{Bu}_2(\text{S})\text{P-P-P-}t\text{Bu}_2$) or phosphinidene ($t\text{Bu}_2\text{P-P-P}$) ligands.